water

MDPI

Article

Potential of Decentral Nature-Based Solutions for Mitigation of Pluvial Floods in Urban Areas—A Simulation Study Based on 1D/2D Coupled Modeling

Jonas Neumann *, Christian Scheid and Ulrich Dittmer

Department of Urban Water Management, Institute Water Infrastructure Ressources, University Kaiserslautern-Landau (RPTU), Paul-Ehrlich-Str. 14, 67663 Kaiserslautern, Germany; christian.scheid@rptu.de (C.S.); ulrich.dittmer@rptu.de (U.D.)
* Correspondence: jonas.neumann@rptu.de

Abstract: Urban drainage systems are generally designed to handle rainfall events only up to a certain intensity or volume. With climate change, extreme events that exceed the design storms and consequently result in flooding are occurring more frequently. Nature-based solutions (NBSs) have the potential to reduce the pressure on urban drainage systems and to increase their resilience. This study presents an approach to compare and evaluate the effectiveness of NBSs for flood mitigation using a coupled 1D/2D model of surface and sewer flow. The study analyzes the effect of infiltration systems (dimensioned to return periods of T = 5 and 100 years), various green roofs, and tree pits considering the different degrees of implementation. The NBSs are represented as LID elements according to SWMM. As expected, the mitigation effect of NBSs declines with increasing rainfall intensities. However, infiltration systems dimensioned to T = 100 years achieve almost three times the flood reduction compared to systems dimensioned to T = 5 years, even during extremely heavy rainfall events (100 mm), resulting in a reduced total flood volume of 15.1% to 25.8%. Overall, green roofs (excluding extensive green roofs) provide the most significant flood reduction (33.5%), while tree locations have the least effect.

Keywords: NBS; SWMM LID; 1D/2D flood modeling; flood mitigation; infiltration systems; swales; green roofs; tree trenches

Citation: Neumann, J.; Scheid, C.; Dittmer, U. Potential of Decentral Nature-Based Solutions for Mitigation of Pluvial Floods in Urban Areas—A Simulation Study Based on 1D/2D Coupled Modeling. *Water* **2024**, *16*, 811. https://doi.org/10.3390/w16060811

Academic Editors: Luca Giovanni Lanza and Arianna Cauteruccio

Received: 25 January 2024
Revised: 3 March 2024
Accepted: 6 March 2024
Published: 8 March 2024

1. Introduction

The adverse effects of climate change, such as the rise in heavy rainfall events [1,2], disproportionately affect cities. Increased surface sealing exacerbates runoff, resulting in flooding. With around 57% of the global population living in cities (83% in North America and 75% in Europe) [3], the number of people affected is very high and ever-increasing. It is expected that by 2030 this figure will be 60% [4]. In addition to the risk to life, there is also the economic damage caused by flooding due to the high accumulation of tangible assets in cities. Urban drainage systems are traditionally gray infrastructure that convey stormwater out of urban areas [5]. However, they cannot be dimensioned for extreme rainfall events for technical and economic reasons [6]. Thus, there is a need to improve the resilience of existing urban drainage systems against extreme heavy rainfall events [7].

The problems mentioned above are considered to be mitigated by nature-based solutions (NBSs). NBSs describe both natural and engineered systems that use and enhance physical, chemical, and microbiological treatment processes [8]. According to the European Commission, they are inspired by nature, cost-efficient, and promote resilience towards the impacts of climate change [9]. From an urban drainage perspective, there are several other names for NBS, including sustainable urban drainage systems (SUDS), low-impact development (LID), and blue-green infrastructure (BGI), to name a few [5]. NBSs can be categorized into central and decentral NBSs. Central NBSs are incorporated in the drainage

system, for example, a rainwater retention basin at the outlet of a catchment. Decentral NBSs are located at the source of the runoff before it enters the drainage system and are widespread over the study area. In this study, decentral NBSs are investigated and referred to as just NBSs in the following Sections. Examples of measures are infiltration swales, green roofs, and the unsealing of paved surfaces, which promote infiltration and storage and delay stormwater runoff. Other positive effects are the reduction in heat stress through evapotranspiration and the increase in biodiversity [10,11]. The existing urban drainage system can be retrofitted with NBSs, which retain or delay the runoff before entering the sewer and thus improve the resilience of the drainage system.

The effectiveness of NBSs in retaining or detaining stormwater depends on their physical processes, such as infiltration, evaporation, or delayed outflow, and the system's effective storage volume. Currently, there are no standardized design regulations for the dimensioning of NBSs internationally. The guidelines in Great Britain, Switzerland, and the USA propose dimensioning infiltration systems like swales to a rainfall event with a 10-year return period, Germany to a 5-year return period, and Australia to a 2-year return period [12]. The contribution of infiltration systems to flood reduction in extreme heavy rainfall events should be analyzed, particularly when they are dimensioned above their normal design level.

To assess the performance of NBSs in flood reduction, mainly models are used due to the lack of data from actual field measurements or other data [13]. The Storm Water Management Model (SWMM) [14] is widely used for the representation of NBSs with their LID elements [15,16]. Numerous studies have utilized the observed data from experimental NBSs to validate and calibrate the LID model approach in SWMM [17–19]. In addition to the NBSs, the catchment must be modeled. The primary model approaches in urban drainage are 1D, 2D, or 1D/2D coupled models. However, 1D models cannot simulate the flooding on the 2D surface [16], whereas 2D models do not consider the drainage systems. Dual-drainage concepts as 1D/2D coupled models provide the most detailed representation of an urban catchment with its topography, path-modifying elements (buildings, curbs), and sewer system [20,21].

Several modeling studies have investigated the effect of NBSs on flood reduction [16,22–28]. The study areas varied in scale (regional, city, or catchment), topography, drainage system capacity, and infiltration characteristics of the soil. Different modeling approaches were used to represent the study areas and NBSs. Additionally, there are currently no internationally standardized design regulations for NBSs. Overall, the effectiveness of NBSs in flood reduction is highly dependent on the specific case, which limits the comparability of results between studies. It is advantageous to compare and evaluate the performance of different types of NBSs for flood mitigation within the same study.

In many studies, researchers simulated only one scenario with different combinations of NBS types and compared them to the base model without an NBS [16,22–24]. This approach makes it impossible to quantify the effect of individual NBS types on flood reduction. To address this issue, different scenarios are needed.

In their study, Bai et al. [25] compared the reductions in runoff for three scenarios: LID types based on infiltration, LID types based on water storage, and a combination of both types. The study provides information on the total area occupied by the infiltration LID and the total storage volume of the storage LID. However, the impervious area connected to the LID based on infiltration is not mentioned. A comparison of flood reduction between LID types can be made, but it is difficult to evaluate the effect of the LID types without a relation to the connected impervious area. Costa et al. [26] investigated the effect of grid pavements, green roofs, and water storage on the streets in six different scenarios. However, due to model shortcomings, the grid pavements and green roofs were simulated by disconnecting them completely. A more realistic representation of the NBSs is needed to compare and evaluate their effect on flood mitigation. Webber et al. [27] simulated several scenarios, including two where all roofs were designed as green roofs, respectively, connected to rainwater harvesting tanks. This allowed for the better comparison and evaluation of

flood mitigation performance because the same amount of impervious area was connected. However, the NBSs were implemented by editing the rainfall input for the areas occupied by the NBSs, neglecting the underdrain of the green roofs. Mugume et al. [28] investigated the effectiveness of detention ponds, infiltration trenches, rainwater harvesting systems, and bioretention cells in different scenarios. The NBS types were modeled individually, but the total NBS storage volume was kept identical for all scenarios. This approach enables a comparative evaluation of the effectiveness of NBS in reducing floods. Additionally, they conducted a cost–benefit analysis expressing the benefits of NBSs in monetary terms. More research is needed for comparing and evaluating the effect of other types of NBSs for flood mitigation.

This study presents a method to implement NBSs in a 1D/2D coupled model to quantify their effectiveness in flood mitigation in a densely populated catchment. The effect of different infiltration systems, green roofs, tree trenches, and tree pits is compared and evaluated based on design rains with varying return periods, durations, and rainfall distributions. In addition, the influence of the spatial distribution of NBSs in the study area is investigated.

2. Materials and Methods

2.1. Study Area and 1D/2D Model

The study area, situated in the heart of Berlin, Germany, has a predominantly flat topography and spans approximately 3.4 km^2. Figure 1 shows the catchment area, delineated by its sewer catchment and in the north, east, and south by bodies of water. The highly urbanized area comprises 0.98 km^2 roofs, 0.76 km^2 streets, 0.62 km^2 yard and walk or bikeways, and 1.03 km^2 of pervious green area. Also, the natural soil is medium sand with a high infiltration capacity, and there are 3256 street trees located in the study area.

A 1D/2D surface runoff model was created for the study area using the software InfoWorks ICM (version 2023.2). The 1D sewer model was provided by Berlin's municipal water services (Berliner Wasserbetriebe (BWB), Berlin, Germany). It is a combined sewer system comprising 1382 manholes, 1619 conduits, 1 pumping station, and 19 stormwater overflows. In addition, the BWB provided the location of 1801 street inlets, which were integrated into the model. The street inlets and the manholes act as coupling points between the 1D sewer and the 2D surface model.

The 2D surface model was set up using open geo data from the geoportal of Berlin (FIS-Broker) from the Senate Department for Urban Development, Building, and Housing [29]. It is based on the digital elevation model with a resolution of 1 m^2 (DEM1). As impervious surfaces, the street and yard as well as the walk- and bikeway areas are modeled in 2D, and the rainfall is applied directly to them. The roof areas are modeled as subcatchments connected to the nearest manhole. Table 1 lists the impervious surfaces with their corresponding discharge and roughness coefficients. The discharge coefficients are based on the recommended values from the German guideline DWA-A 138-1 [30] for the dimensioning of infiltration systems; the roughness coefficients are obtained from the literature [31]. The roof area has no roughness coefficient because it is modeled as a subcatchment, not a 2D surface.

Table 1. Runoff and roughness coefficients of the impervious surfaces.

Area [-]	Discharge Coefficient [-]	Roughness Coefficient n [$s \cdot m^{-1/3}$]
Roofs	1.0	-
Streets	0.97	0.0143
Yards and walk/bikeways	0.85	0.02

Figure 1. Study area in the center of Berlin.

All other areas are defined as pervious. It is assumed that this pervious area is a green space. The soil type in the entire study area is medium sand so that the infiltration process can be modeled with one set of parameters. The infiltration of the green space with medium sand as natural soil is modeled using the Horton infiltration approach, whereby the following parameters are used:

- Initial infiltration rate: 127 mm/h;
- Final infiltration rate: 8.34 mm/h;
- Decay constant: 64 1/h.

The roughness coefficient of the green area is selected as n = 0.0286 s · $m^{-1/3}$, the value for green space in urban areas according to Hürter [31].

The 1D/2D model without an NBS described here would be referred to as the base model in the following.

2.2. Description and Dimensioning of the Decentral NBS

Figure 2 shows the various investigated decentral NBSs. They are categorized into infiltration systems (swale, infiltration trench, swale–trench–element), green roofs (intensive and extensive green roof, retention roof), and tree locations (tree pit, tree trench).

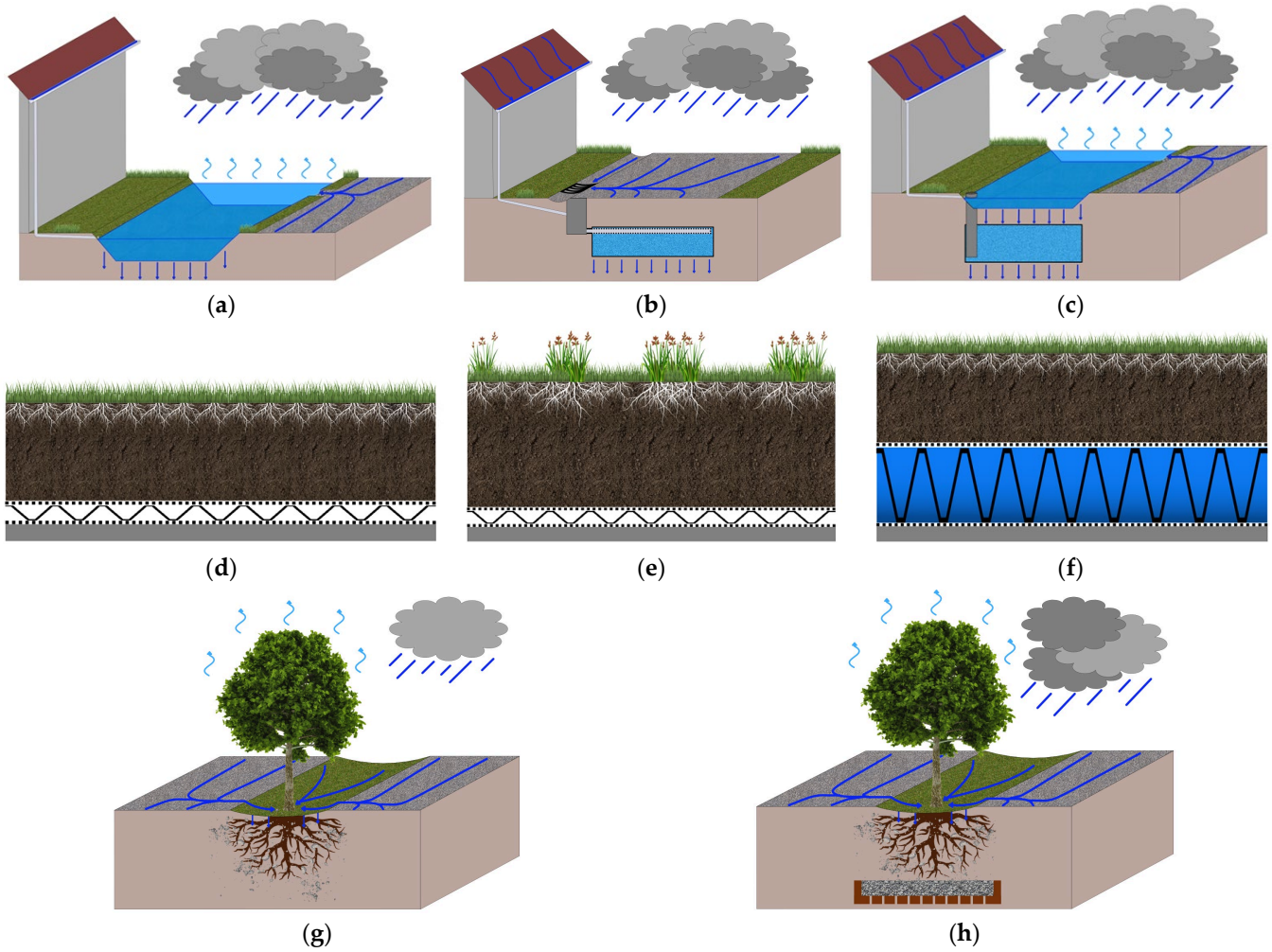

Figure 2. Investigated decentral NBSs. Infiltration systems: (**a**) swale; (**b**) infiltration trench; (**c**) swale–trench–element; green roofs: (**d**) extensive green roof; (**e**) intensive green roof; (**f**) retention roof; tree locations: (**g**) tree pit; and (**h**) tree trench.

In a swale, stormwater runoff from impervious surfaces, such as roofs and streets, is collected and infiltrated through the natural soil. The infiltration trench is an underground storage for stormwater runoff, from where the stormwater exfiltrates in the soil. The swale–trench–element is a combination of a swale with an infiltration trench underneath [32]. In this element, the overflow from the swale bypasses the soil layer and enters the infiltration trench directly via a pipe.

Extensive green roofs have low-maintenance vegetation like moos, succulents, and grass. Under the comparatively thin substrate layer is a drainage layer. Intensive green roofs can be vegetated with a large variety of plants: simple grass, shrubs, or even small trees. The substrate layer is bigger, and a drainage layer is underneath. Retention roofs can be designed as either extensive or intensive green roofs: the special feature is the retention layer under the substrate layer, in which stormwater is stored in a porous medium.

The stormwater runoff from adjacent roads and sideways in a tree pit is channeled directly to the tree grid. In addition, a tree trench has an infiltration trench at the bottom of the planting pit [33].

2.2.1. Dimensioning of the Infiltration Systems

In the first step, the infiltration systems were pre-designed for a 5- and 100-year return period according to the German DWA guideline DWA-A 138-1 [30]. The systems were implemented into the model with the determined areas from the pre-design. The system

areas were adjusted based on simulation results with the aim that an overflow from the system only occurs for a rainfall load with a return period higher than the return period from the pre-design. Table 2 lists the final dimensions of the infiltration systems.

Table 2. Final dimensions of the infiltration systems; A_{im}: connected impervious area (100% runoff), H_S: height of the swale, H_{IT}: height of the infiltration trench, A_{IS}: area of the infiltration system, and A_{IS}:A_{im}: ratio between area of the infiltration system and connected impervious area.

Infiltration System	Return Period [a]	A_{im} [m^2]	H_S [m]	H_{IT} [m]	A_{IS} [m]	V_{IS} [m^3]	A_{IS}:A_{im} [%]
Swale	5	1000	0.3	-	66.2	19.86	6.62
	100	1000	0.3	-	138.2	41.46	13.82
Infiltration trench	5	1000	-	0.6	38.2	22.92	3.82
	100	1000	-	0.6	75.6	45.36	7.56
Swale–trench–element	5	1000	0.3	0.331	39.5	24.92	3.95
	100	1000	0.3	0.523	83.3	32.51	8.33

The A_{IS}:A_{im} ratio is the main output: it is the ratio between the area of the infiltration system and the connected impervious area of 1000 m^2. This ratio can be used to calculate the required area of infiltration systems depending on the connected impervious area:

$$A_{IS} = (A_{IS}:A_{im}) \cdot 0.01 \cdot A_{IM} \quad (1)$$

However, this only applies to this study area with its specific rainfall data and soil properties.

2.2.2. Structure of the Green Roofs

In contrast to infiltration systems, green roofs are not designed to manage specific storm events. The effect on stormwater runoff is not a design goal. There are a variety of combinations of vegetation, soil layer substrate, and thickness, as well as drainage elements. For this reason, a representative structure is defined for each of the three types of green roofs—extensive, intensive, and retention roofs (Table 3). The structures are mainly based on recommendations from the German guideline for green roofs [34].

Table 3. Representative structure of the selected green roofs; EGR: extensive green roof, IGR: intensive green roof, and RR: retention roof.

Layer	Thickness [mm]			Description
	EGR	IGR	RR	
Vegetation	-	-	-	Moos, succulent, and grass vegetation for EGRs and RRs; grass and shrubs for IGRs
Soil	100	300	150	Vegetation substrate for multi-layer green roofs
Filter fleece	10	10	10	Fleece to protect the drainage/retention layer
Drainage/retention	25	25	125	Drainage elements made of hard plastic
Protective fleece	15	15	15	Fleece to protect the roof waterproofing

2.2.3. Structure and Dimensioning of Tree Pits and Tree Trenches

Contrary to the other NBSs, the system size of the tree pits and the tree trench are not adjusted based on the connected impervious area. Instead, a standard setup is defined for both systems, and the connectable impervious area is adjusted. The reason for this is the boundary conditions: A minimum volume of the planting pit must be provided for the tree's development, and the system's size must not fall below this volume. The maximum volume of the planting pit is also restricted due to the limited space available in the street where the tree locations are located.

The structure of the tree locations (Table 4) are based on the recommendations and practical experience on vital tree sites from the BlueGreenStreets project [33]. The dimensions of the tree pit (6 m^2 tree grid area, 9 m^2 planting pit area, and 13.5 m^3 planting pit volume) and the tree trench (6 m^2 tree grid area, 9 m^2 planting pit area, and 18.9 m^3 planting pit volume) are based on the recommendations of the German guideline for tree plantings [35].

Table 4. Structure of the tree pit and the tree trench.

Tree Location	Layer	Thickness [cm]	Description
Tree pit	Tree grid	5	Swale-shaped tree grid
	Tree substrate	40	Replaced substrate with a pore volume of 35%
	Existing soil	110	Existing soil up to 1.5 m depth with a pore volume of 20%
Tree trench	Tree grid	20	Swale-shaped tree grid
	Tree substrate	150	Optimized tree substrate with a pore volume of 25%
	Infiltration trench	30	Infiltration trench (sand/split/gravel) with a pore volume of 30%
	Storage	30	Storage (sand/gravel) with a pore volume of 30%, sealed (not completely) by, e.g., clay

The tree pit and tree trench were implemented in the model with the standard setups and simulations described here being carried out while adjusting the connected impervious area. The calibration goal was that an overflow out of the tree locations only occurs from a rainfall load with a return period higher than T = 5 a. The calibration goal for the tree pit is achieved when 78 m^2 of impervious area is connected. For the tree trench, the goal is achieved when 120 m^2 is connected. When connecting more impervious area, an overflow already occurs for the 5-year rain event.

2.3. Modeling of the NBSs and Model Parameters

2.3.1. Model Approach

The simulation software InfoWorks ICM models NBSs as sustainable urban drainage system (SUDS) elements, utilizing the low-impact development (LID) objects from SWMM and employing a similar model approach. These SUDS elements feature a horizontal layer structure. Figure 3 illustrates a bio-retention cell with its associated layers, serving as a generic example of a SUDS element. For detailed modeling approaches for each layer, refer to Rossman and Huber [36].

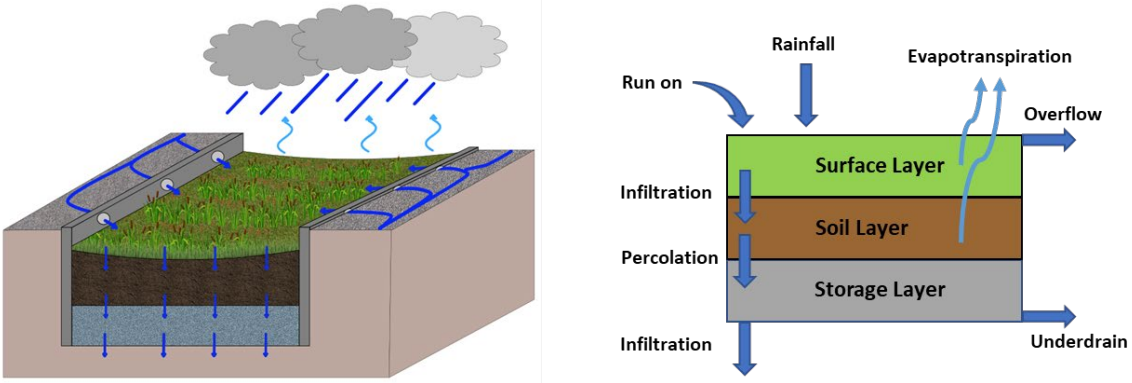

Figure 3. Layer structure of the SUDS element bio-retention cell in InfoWorks ICM/SWMM (own illustration based on Rossman and Huber [36]).

Table 5 outlines the studied NBSs and their portrayal in the model as SUDS elements and their respective layers. The swale–trench–element is depicted as an infiltration trench comprising the surface and storage layers. Notably, the model excludes the representation of the soil layer, bypassing it during extreme events. Consequently, water infiltrates directly into the infiltration trench, with ponding in the swale occurring only after the infiltration trench reaches full capacity.

Table 5. NBS and SUDS elements with the corresponding layers.

NBS	SUDS Element	Layer			
		Surface	Soil	Storage	Drainage Mat
Swale	Rain garden	x	x	-	-
Infiltration-trench	Rain barrel	-	-	x	-
Swale–trench–element	Infiltration trench	x	-	x	-
Intensive green roof	Green roof	x	x	-	x
Extensive green roof	Green roof	x	x	-	x
Retention roof	Bio-retention cell	x	x	x	-
Tree pit	Rain garden	x	x	-	-
Tree Trench	Bio-retention cell	x	x	x	-

The retention roof is modeled with the SUDS element bio-retention cell. This allows for the integration of a storage layer.

In all cases of NBSs, the evaporation process is neglected due to the focus of this study on short, intense, and heavy rainfall events.

2.3.2. Model Parameters

Table 6 lists the selected model parameters and layers for NBSs. The swale's soil parameters are the standard sand parameters of InfoWorks ICM/SWMM [37]. The storage layer of the infiltration trench has a storage void ratio of 9, corresponding to a pore volume of 90%. The seepage rate of 120.4 corresponds to the hydraulic conductivity of the soil sand.

The model parameters of the green roofs were chosen based on studies by Peng and Stovin and Jeffers et al., which compared the results from experimental green roof setups with SWMM simulation results and calibrated the model parameters [38,39].

2.4. Integration of the NBSs in the 1D/2D Model

2.4.1. Implementation of the NBS

Scenarios with varying degrees of NBS implementation were modeled and evaluated. In all scenarios, only roof areas were connected to infiltration systems, while streets and sidewalks were connected to tree pitches and tree trenches. Only roofs and no other impervious areas are connected to infiltration systems due to the 1D/2D model approach: the roofs are already implemented as 1D subcatchments. They can be easily modified to represent infiltration systems or green roofs. Other impervious areas like courtyards are modeled in 2D. To connect them to an infiltration system, they must again be inserted into the model as a 1D subcatchment, which is very time-consuming.

The infiltration systems are incorporated into the roof subcatchments. This has the great advantage that no additional subcatchment has to be modeled for each roof. In the case of swales or swale–trench–elements, the infiltration area is added to the connected roof to consider the precipitation on the swale. The roof area does not need to be enlarged for infiltration trenches because they are underground and not exposed to precipitation. The overflow from infiltration systems and trees, as well as the underdrain of green/retention roofs, is connected to the sewer system via the nearest manhole.

Table 6. Model parameters; S: swale, IT: infiltration trench, STE: swale–trench–element, EGR: extensive green roof, IGR: intensive green roof, RR: retention roof, TP: tree pit, and TT: tree trench.

Layer	Parameter	Unit	Infiltration Systems			Green Roofs			Tree Locations	
			S	IT	STE	EGR	IGR	RR	TP	TT
Surface	Berm height	[mm]	300	-	300	10	10	10	33.3	133.3
	Vegetation volume fraction	[vol fr.]	0.1	-	0.1	0.1	0.2	0.1	0.1	0.1
	Surface roughness	$[s \cdot m^{-1/3}]$	0.2	-	0.2	0.2	0.5	0.2	0.2	0.2
	Surface slope	[m/m]	0.02	-	0.02	0.02	0.02	0.02	0.02	0.02
Soil	Soil thickness	[mm]	500	-	-	110	310	160	1500	1500
	Soil porosity	[vol fr.]	0.437	-	-	0.45	0.45	0.45	0.24	0.24
	Field capacity	[vol fr.]	0.062	-	-	0.3	0.3	0.3	0.190	0.190
	Wilting point	[vol fr.]	0.024	-	-	0.05	0.05	0.05	0.085	0.085
	Conductivity	[mm/h]	120.4	-	-	881	881	881	180	180
	Conductivity slope	[-]	48	-	-	50	50	50	55.4	55.4
	Suction head	[mm]	49.0	-	-	110	110	110	110	110
	Seepage rate	[mm/h]	120.4	-	-	-	-	-	120.4	-
Storage	Storage thickness	[mm]	-	600	331/523 *	-	-	125	-	600
	Storage void ratio	[-]	-	9	9	-	-	9	-	0.429
	Seepage rate	[mm/h]	-	120.4	120.4	-	-	0.5	-	12.04
	Storage clogging factor	[-]	-	0	0	-	-	0	-	0
	Coefficient for flow	[mm/h]	-	0	0	-	-	200	-	26.68
	Flow exponent	[-]	-	0	0	-	-	0	-	0
	Offset height	[mm]	-	0	0	-	-	100	-	300
Drainage mat	Mat thickness	[mm]	-	-	-	25	25	-	-	-
	Mat void fraction	[vol fr.]	-	-	-	0.6	0.6	-	-	-
	Mat roughness	$[s \cdot m^{-1/3}]$	-	-	-	0.03	0.03	-	-	-

* Storage thickness of 331 mm for the dimensioning with a return period of T = 5 a and of 523 mm for a return period of T = 100 a.

The modeling approach slightly overestimates the runoff from the green areas as the precipitation on swales is considered twice: on the added virtual infiltration area in the roof subcatchment and on the green space where the swale would typically be located. For the swales dimensioned to T = 5 a and an implementation degree of 100%, the additional precipitated green area is 6.5 ha, corresponding to an increase of 6.3%.

The maximum street area that can be connected to a tree pit is 78 m^2 and 120 m^2 to a tree trench. For the implementation in the model, the street area is divided into 78 m^2 or 120 m^2 polygons. The locations of the street trees in the study area are known (3256 in total). Figure 4 shows a street section divided into 120 m^2 polygons and the location of street trees. It is assumed that each street tree can be converted into a tree pit or a tree trench. The polygons containing a street tree are selected and imported as subcatchments into the model. The subcatchments are connected to the corresponding tree locations, defined as tree trenches. Rain falling on subcatchments is conveyed to the tree location and not applied to the 2D surface. Runoff from a 2D surface without an overlaying subcatchment can still flow to an adjacent street area with a subcatchment, as the underlying infiltration zone continues to represent the 2D surface (though not directly rained on).

2.4.2. Spatial Distribution of the NBSs

Concerning the spatial distribution of NBSs, heterogeneous and homogeneous scenarios were considered. Figure 5 illustrates a scenario using the example of green roofs with a degree of implementation of 50%. In the heterogeneous scenario, 50% of the roofs are converted into green roofs. In the homogeneous scenario, 50% of each roof area is designed as green. This approach allows the change in the degree of implementation in the study area at one time without selecting individual roofs manually. The two approaches are transferable to the other NBSs.

(**a**) (**b**)

Figure 4. (**a**) Street area divided into 120 m^2 polygons (blue) and the locations of street trees (green); (**b**) selected polygons that represent subcatchments connected to a tree trench in the model.

(**a**) (**b**)

Figure 5. (**a**) Heterogenous distribution of the green roofs: 50% of the roof areas implemented as green roofs; (**b**) homogeneous distribution: 50% of each individual roof area is designed as a green roof.

2.5. Rainfall Data and Model Configurations

Design rains with different return periods and rainfall distribution were used. Table 7 shows the characteristics of the selected rainfall events. Block rains with return periods of 5 and 100 years and a duration of 60 min (R0B and R1B) were used to dimension the infiltration systems and the tree locations. According to the data [40] published by the German Weather Service (Deutscher Wetter Dienst), the corresponding precipitation heights are 25 mm (R0B) and 48.9 mm (R1B) in the study area (Appendix A Table A1). For the effect evaluation of the NBSs in flood mitigation, Euler type 2 rainfall distribution (R1E and R2E) was selected. Figure 6 shows the Euler type 2 rainfall distribution compared to block rain for R1E and R1B: the amount of precipitation is the same, just distributed differently. The Euler type 2 rainfall distribution is the standard design rain in Germany. In addition to R1E, a rainfall event with the same return period but a duration of 6 h (R1E6) and an extreme rainfall event with a precipitation height of 100 mm (R2E) were selected.

Table 7. Characteristics of rainfall events.

Name [-]	Rainfall Distribution	Return Period [a]	Duration [min]	Precipitation Height [mm]
R0B	Block rain	5	60	25
R1B	Block rain	100	60	48.9
R1E	Euler type 2	100	60	48.9
R1E6	Euler type 2	100	360	74.3
R2E	Euler type 2	>>100	60	100

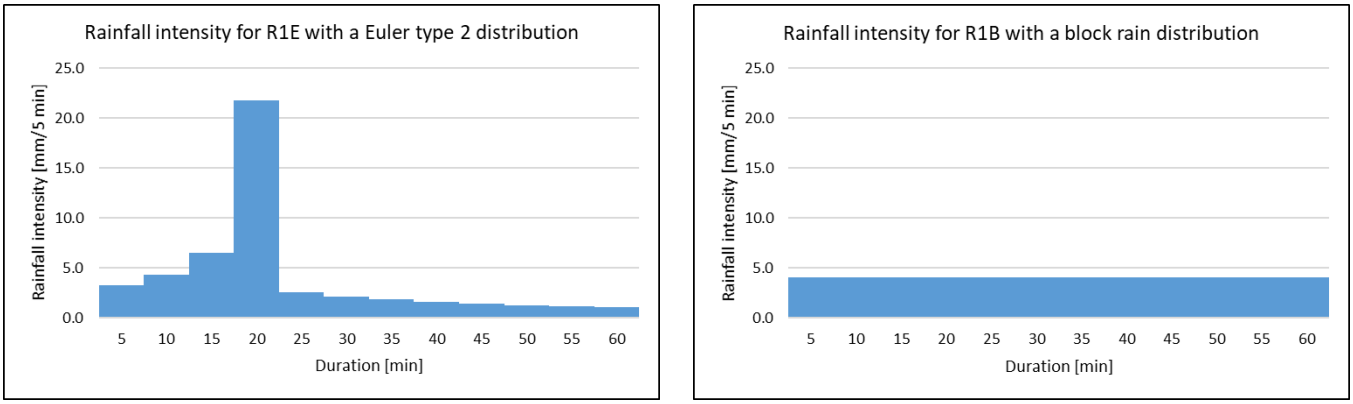

(**a**) (**b**)

Figure 6. (**a**) Euler type 2 rainfall distribution; (**b**) block rain distribution.

In total, 106 simulations were carried out. The simulation runs are composed of 104 runs with the homogenous spatial distribution of NBSs (Appendix A Table A2) and 2 with the heterogenous distribution. The simulations with a considered period of 75 min were carried out on a PC with a 6-core CPU (i5-9600k), 32 GB RAM (DDR4), and a dedicated GPU (RTX 2070). The simulation duration of each individual run was between 2.5 and 3 h, with the 1D/2D model consisting of 1,744,349 mesh elements.

3. Results

The simulation results of the base model and the models with NBSs are compared to assess the effect of NBSs on flood reduction. The flood volume is calculated from the maximum water level in each mesh element and the area of the associated mesh element (approximately 1 m^2 in size). The total flood volume in the study area is calculated as the sum of all affected mesh elements. Only potentially hazardous water levels of 10 cm or more are considered. The reduction in total flood volume is chosen as the main criterion to compare the effectiveness of the NBSs because it incorporates the decreases in inundation heights and flood extent in one key figure. Flow velocities are not used for the evaluation as the study area is very flat. In the following Section, the effect of NBSs with a homogenous distribution in the study area is investigated, and the effect of the heterogenous approach is investigated separately in Section 3.4.

3.1. Influence of the Degree of NBS Implementation on Flood Mitigation

The impact of the NBS implementation degree on flood mitigation is demonstrated using swales as an example. Figure 7 shows the total flood volumes in the study area for the base model and different implementation degrees of swales dimensioned for a return period of T = 5 a (Type 5 a) and 100 a (Type 100 a). The diagrams show the results for the design rains R1E and R2E. A degree of implementation of 100% means that all roof areas are completely connected to swales.

In this scenario, swales of Type 5 a reduce the flooding volume of the 100-year design rain R1E (precipitation height: 48.9 mm) by 6.1% to 21.6%, while the swales of Type 100 a reduce it by 12.2% to 33.7%. As expected, the relative reduction is lower in the case of the design rain R2E (precipitation height: 100 mm), with 1.3% to 5.4% for the Type 5 a swales and 3.9% to 15.1% for the Type 100 a swales.

In the case of R1E, the decrease in flood volume is not linear compared to the increase in the implementation degree of swales. Connecting 25% of the roof area to Type 5 a swales results in a 6.1% reduction in total flood volume, while increasing the degree of implementation from 75% to 100% only reduces the volume by 4.4% (from 82.7% to 78.4%). This non-linearity is even more pronounced for the swales of Type 100 a. Connecting 25% of the roof area to such swales results in a 12.2% reduction in total flood volume, while an increase in implementation from 75% to 100% only reduces the volume by 3.6% (from

69.9% to 66.3%). For the less intensive rain R1E, lower degrees of implementation have a comparatively bigger effect on flood reduction. This effect is even more substantial for the Type 100 a swales than the Type 5 a swales. The reason for this is the drainage system's capacity: The system is overloaded, and even with a lower degree of NBSs, runoff that would otherwise flood the surface if there were no NBS can be avoided. The drainage system is less loaded at higher implementation degrees, and the flooding in the study area is already less severe. As a result, an even higher implementation NBS degree does not have a major additional impact.

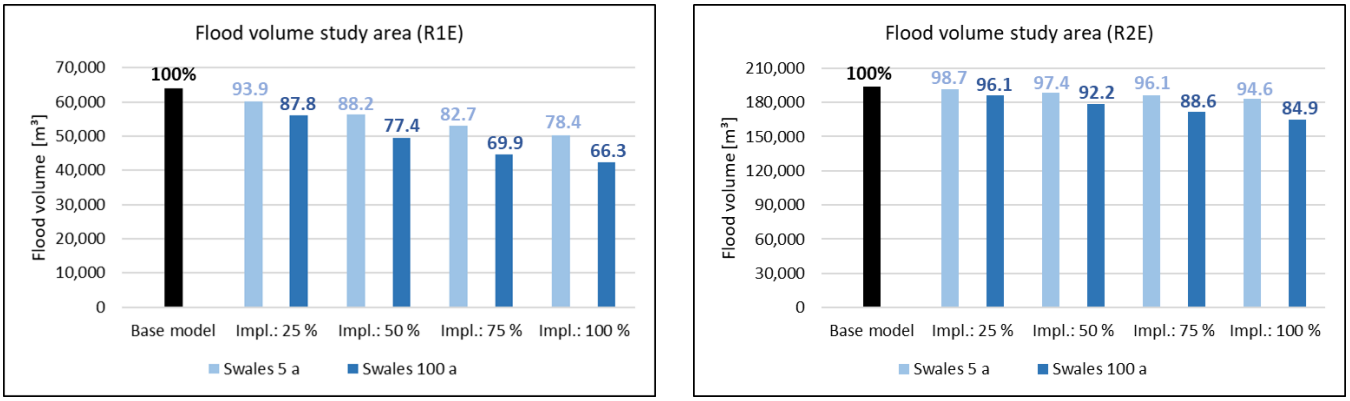

(**a**) (**b**)

Figure 7. Total flood volume in the study area for the base model and with swales (dimensioned to T = 5 and 100 a) with different degrees of implementation: (**a**) total flood volume for R1E (precipitation height: 48.9 mm) and (**b**) total flood volume for R2E (precipitation height: 100 mm).

With the more intensive rain R2E, the correlation between the implementation degrees regarding the reduction in total flood volume is almost linear: For the Type 5 a swales, the reduction is 1.3% at an implementation degree of 25%. Between the 75% and 100% implementation degrees, the reduction is 1.5% (from 96.1% to 94.6%). The reduction in the Type 100 a swales is 3.9% at an implementation degree of 25%. Between the 75% and 100% implementation degrees, the reduction is 3.7% (from 88.6% to 84.9%). For the more intense rain R2E, the degrees of implementation comparatively have almost the same effect on flood reduction.

Figure 8 shows the maximum water levels (flood depths of at least 10 cm) in the center of flooding in the northeast of the study area as a result of R1E, simulated with the base model and for the swales Type 100 a at implementation degrees of 50% and 100%. The comparison shows a significant reduction in flooding when swales are implemented. The black arrows mark the lowest point in the street: here, the maximum water levels are 56 cm for the base model and 46 cm and 28 for the swales Type 100 a with implementation degrees of 50% and 100%. The swales reduce the maximum water level by 10 cm and 28 cm, respectively.

3.2. Effect of the Various NBSs for Flood Mitigation

Table 8 compares the effects of the various NBSs on flood reduction for the design rainfall events R1E and R2E with an NBS implementation degree of 100%. In addition, the total overflow volume for infiltration systems and tree location is listed as the total underdrain volume for green roofs. The sewer overflow volume is the total volume discharged from the manholes and street drains onto the 2D surface during the simulation.

In the rainfall scenario, R1E (T = 100 a), the infiltration systems of Type 5 a reduce the flooding by 21.6% to 24.8%, with the swale–trench–elements achieving the highest reduction. The infiltration systems Type 100 a retain the runoff from the roofs completely, reducing the flood volume by 32.3% to 33.8%.

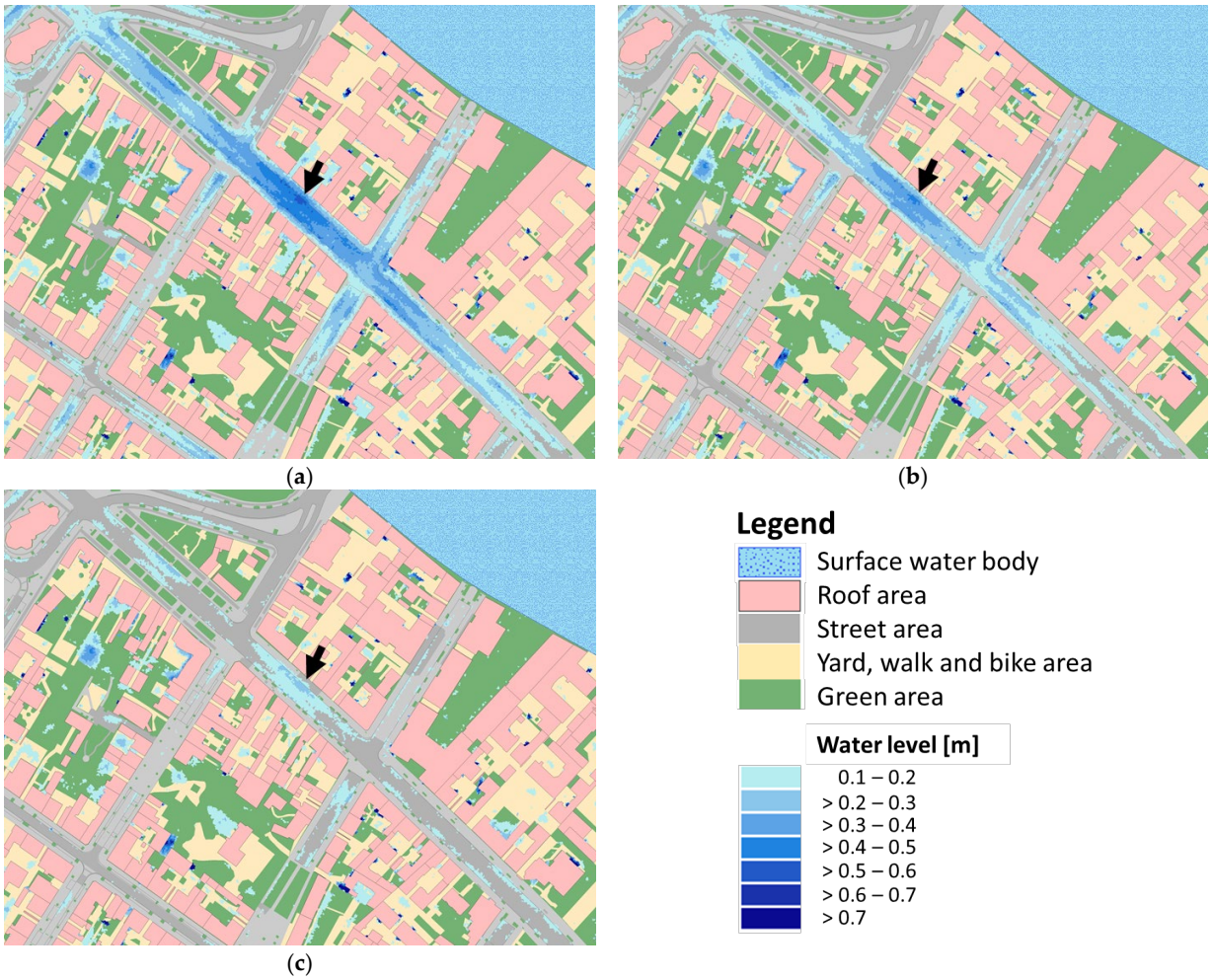

Figure 8. Maximum flood heights in the center of flooding: (**a**) base model; (**b**) swales (T = 100 a), degree of implementation: 50%; and (**c**) swales (T = 100 a), degree of implementation: 100%. The black arrows indicate the lowest point in the street.

Like the infiltration systems of Type 100 a, intensive green roofs and retention roofs retain the rainfall volume of R1E entirely, resulting in the same effect on flood reduction (33.7%). Extensive green roofs have a slightly lower effect on flood reduction (31.8%).

The more extreme rainfall scenario R2E (100 mm in 60 min) exceeds the capacity of all investigated infiltration systems. While the Type 5 a infiltration systems only reduce the flood volume by 5.4% to 9.3%, the Type 100 a systems reduce the flood volume by 15.1% to 25.8%.

The discrepancy in performance can be attributed to the disparity in retention volume, with Type 100 a systems having approximately twice the capacity compared to Type 5 a systems. The effect of the swale–trench–elements is significantly higher compared to the swales and infiltration trenches.

The retention roofs can retain even the rainfall R2E completely, resulting in a flood reduction of 33.6%. This was expected as the storage layer of these roofs already has an effective depth of 90 mm. Intensive green roofs have almost the same effect, with an underdrain volume of only 4200 m^3 reducing the flood volume by 33.5%. The detention capacity of extensive green roofs is clearly exceeded: the 15 cm thick soil layer is fully saturated, and the underdrain drains the water to the drainage system. The effect on flood reduction declines to 13.8%. Compared to the infiltration systems, the performance of the extensive green roofs comes close to the performance of swales Type 100 a. The performance of the intensive green and retention roofs corresponds to a dimensioning of T >> 100 a.

Table 8. Simulation results for R1E and R2E with an NBS implementation degree of 100%.

Model	R1E				R2E			
	Flood Volume [m^3]	Reduction [%]	Overflow or Underdrain [m^3]	Sewer Overflow [m^3]	Flood Volume [m^3]	Reduction [%]	Overflow or Underdrain [m^3]	Sewer Overflow [m^3]
Base model	63,958	-	-	13,859	193,818	-	-	50,300
Swales (T = 5 a)	50,122	21.6	21,947	4422	183,273	5.4	74,661	42,116
Swales (T = 100 a)	42,398	33.7	0	53	164,641	15.1	50,418	27,824
Infiltration trenches (T = 5 a)	50,067	21.7	20,859	4324	181,988	6.1	70,829	41,532
Infiltration trenches (T = 100 a)	43,290	32.3	0	326	162,744	16.0	44,444	27,174
Swale–trench–elements (T = 5 a)	48,071	24.8	19,542	3034	175,776	9.3	66,257	36,147
Swale–trench–elements (T = 100 a)	42,368	33.8	0	48	143,814	25.8	29,435	13,540
Extensive green roofs	43,651	31.8	14,945	658	167,052	13.8	64,396	32,258
Intensive green roofs	42,393	33.7	0	51	128,917	33.5	4200	2948
Retention roof	42,393	33.7	0	51	128,785	33.6	0	2752
Base model tree pits	64,786	-	-	18,717	195,860	-	-	65,024
Tree pits	61,972	4.3	5982	16,452	192,817	1.6	18,536	61,906
Base model tree trenches	64,757	-	-	21,509	196,316	-	-	73,641
Tree trenches	60,256	7.0	9128	17,688	191,915	2.2	28,607	69,027

The tree locations have the least effect on flood mitigation, with only 4.3% and 7.0% for R1E. However, it must be taken into account that there is a much less impervious area connected to the tree pits (25.4 ha street area) and tree trenches (39.1 ha street area) compared to the other NBSs (97.8 ha roof area). Concerning the space required, a tree pit reduces the flood volume by 1.47%/ha (system area), a tree trench by 2.34%/ha, and swale Type 5 a by 3.34%/ha. For the rainfall scenario R2E, the reduction in flooding is negligible for the tree pits at 1.6% and the tree trenches at 2.2%.

3.3. Influence of the Rainfall Characteristics

This Section analyses the influence of rainfall distribution and rainfall duration on the effectiveness of NBSs for flood mitigation.

Figure 9 compares the total flood volume for the base model and various NBSs (implementation degree: 100%), comparing the Euler type 2 and block rain distribution for R1E, respectively, with R1B. The chosen rainfall distribution strongly influences the simulated flood volume: the percentage difference is between 17.8% and 31%, with the base model showing the most significant difference. The difference in the results of the two rainfall scenarios is in the same order of magnitude as the effects of NBSs.

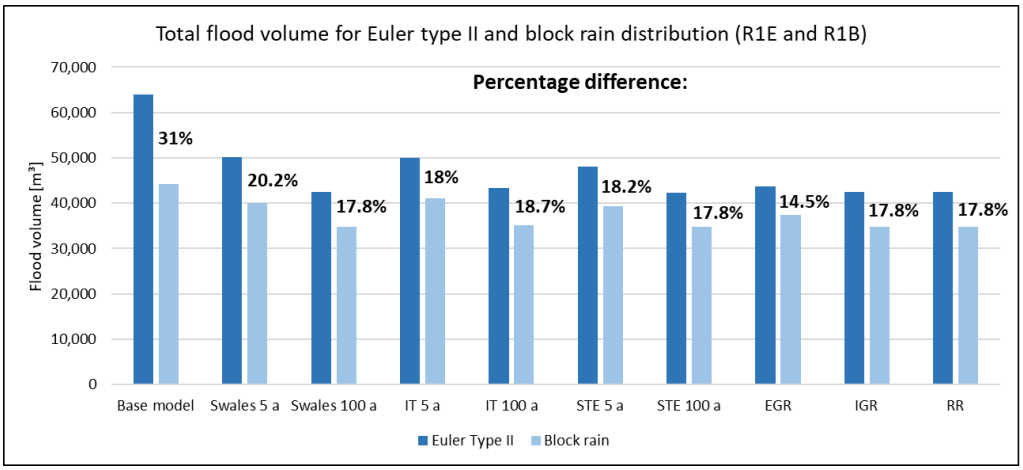

Figure 9. Comparison of the total flood volume for the base model and various NBSs (implementation degree: 100%) between the Euler type 2 and block rain distribution for R1E and R1B, respectively.

The pronounced intensity peak of the Euler type 2 rain leads to higher maximum flood levels, which is crucial for calculating the total flood volume (maximum flood height occurred during simulation multiplied with the corresponding mesh element). For the infiltration system Type 5 a, the percentage difference between the rainfall distributions is 18% to 20.2% compared to the system Type 100 a, with differences of 17.8% to 18.7%. The percentage difference is slightly less for the system dimensioned to T = 100 a. This is because even for Euler type 2 distribution, the flooding is not so severe because of the NBS implementation degree of 100%. Therefore, the difference in flood volumes between Euler type 2 and block rain percentagewise is lower. The same effect occurs in the intensive green and retention roofs simulation with no underdrain. The difference between block and Euler rain is only 14.5% for the extensive green roofs.

Figure 10 compares the total flood volume for the base model and various NBSs (implementation degree: 100%) between R1E and R1E6. Both rainfall events have a return period of 100 years, but differ in duration and rainfall amount: R1E has a duration of 60 min and a precipitation height of 48.9 mm, and R1E6 has a duration of 6 h and a precipitation height of 74.3 mm. In percentage terms, the precipitation height of R1E6 is 51.9% higher than that of R1E.

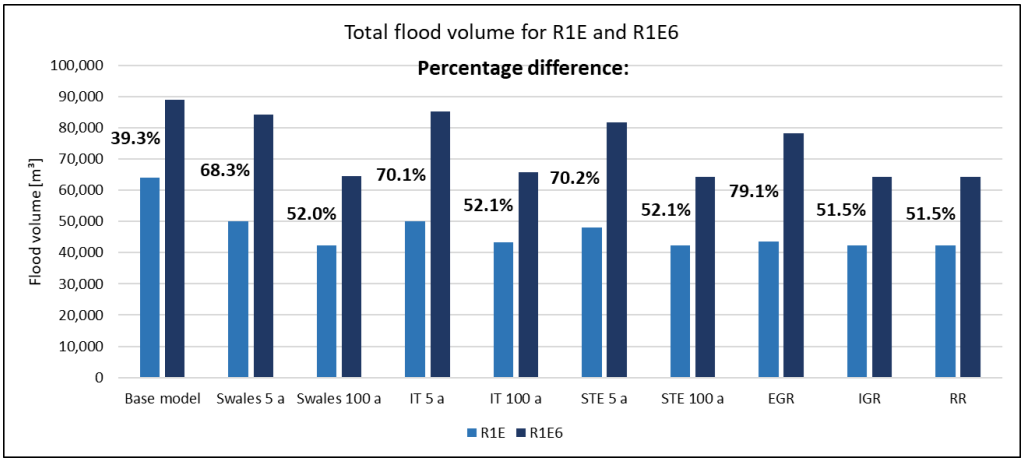

Figure 10. Comparison of the total flood volume for the base model and various NBSs (implementation degree: 100%) between R1E and R1E6.

Overall, the flood volume is much larger for R1E6 compared to R1E. The base model has the smallest percentage difference in flood volume with 39.3%. The percentage difference in flood volume for the infiltration systems Type 5 a is significantly higher with 68.3% to 70.2% compared to the systems Type 100 a with 52.0% to 52.1%. Table 9 lists the inflows and outflows using the example of swales. Due to the longer duration of rain, the infiltration to inflow ratio is much higher for R1E6 compared to R1E, with 55.1% and 85.6% for the Type 5 a and Type 100 a swales, respectively. The influence of the infiltration process increases with infiltration area and rainfall duration.

Table 9. Comparison of the inflows and outflows of the swales for R1E and R1E6.

NBS	Rain	Inflow [m^3]	Infiltration [m^3]	Infiltration/Inflow [%]	Overflow [m^3]
Swales 5 a	R1E	51,005	6478	12.7	21,947
	R1E6	77,458	42,698	55.1	26,053
Swales 100 a	R1E	54,451	12,541	23.0	0
	R1E6	82,689	71,018	85.6	477

The difference in flood volume percentage between R1E and R1E6 is identical for both intensive green roofs and retention roofs, at 51.5%. This corresponds approximately to the percentage difference of the Type 100 a infiltration systems. The extensive green roofs show the highest percentage difference in flood volume among all NBSs, with a value of 79.1%. Their performance collapses completely when the precipitation height exceeds 48.9 mm for R1E. Compared to Type 5 a infiltration systems, they are less robust toward prolonged rainfall because the underdrain drains the runoff in the drainage system instead of infiltrating it into the natural soil like the infiltration systems.

3.4. Influence of the Spatial Distribution of the NBSs

So far, the results have all been simulated with the homogenous distribution of NBSs in the study area. The following addresses the effect of heterogeneity in the spatial distribution. Figure 11c shows the study area with the center of flooding marked in red. The black polygon marks the area around this flooding hot spot, which contains 50.3% of all roofs. As an example of a heterogeneous distribution, roofs inside the polygon are modeled as retention roofs to 100%. For the homogenous distribution, roofs in the entire study area are converted into retention roofs with an implementation degree of 50.3%.

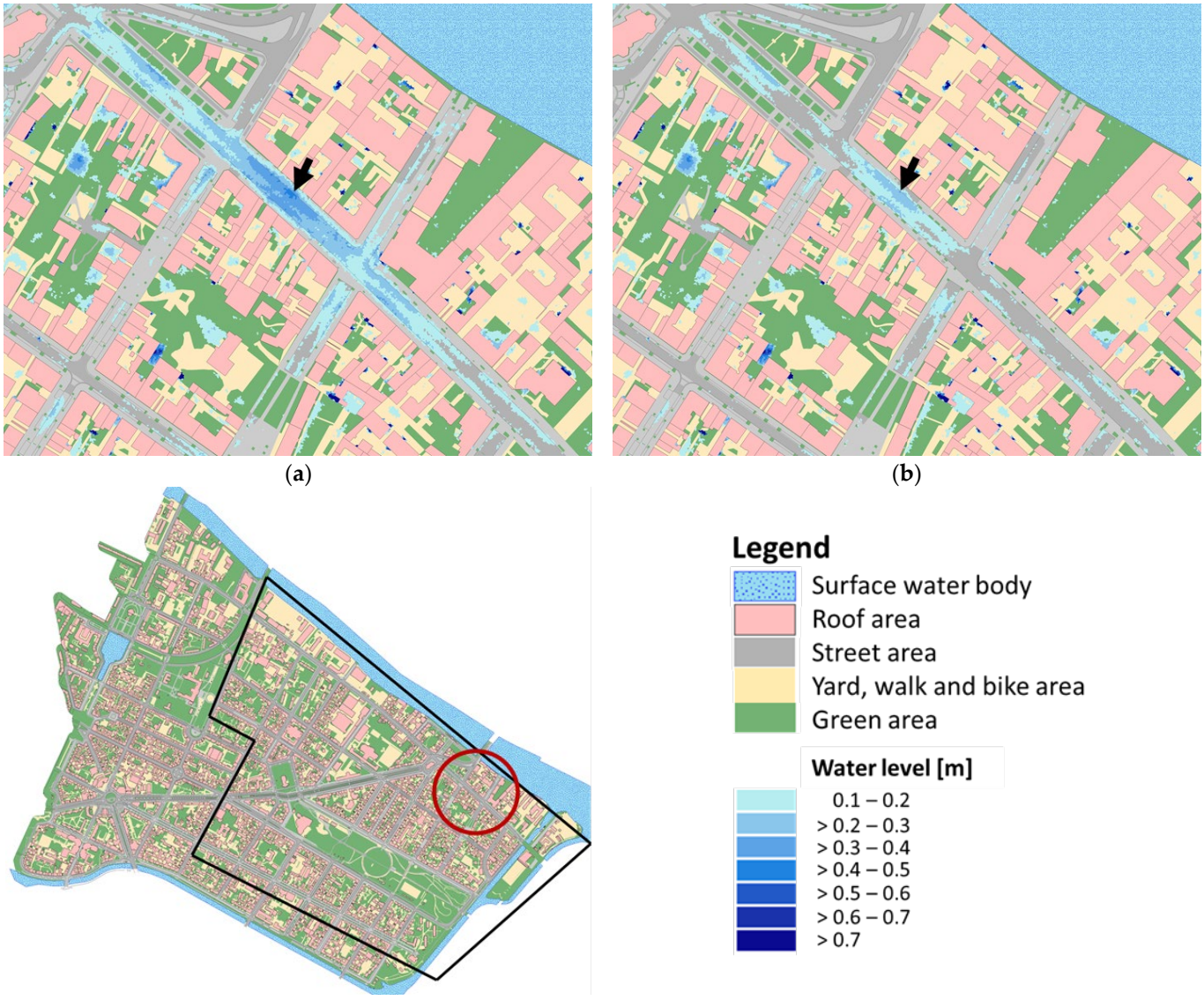

Figure 11. Maximum flood heights in the center of flooding with R1E, and the black arrows indicate the lowest point in the street area: (**a**) homogenous distribution of retention roofs, implementation degree: 50,3%; (**b**) heterogenous distribution of retention roofs, implementation degree: 50.3%; and (**c**) center of flooding marked by a red circle. In the black polygon, 50.3% of the roofs are located.

Figure 11 shows the maximum flood heights in the center of flooding with retention roofs and an implementation degree of 50.3% for the homogenous distribution (a) and the heterogenous distribution (the black arrows indicate the lowest points in the street area) with maximum flood heights of 45 cm (homogenous distribution) and 31 cm (heterogeneous distribution). The difference is much smaller when comparing the flood volume in the entire study area, with 49,411 m^3 for the homogenous and 48,982 m^3 for the heterogenous approach.

4. Discussion

As anticipated, the extent of NBS implementation has the greatest impact on flood reduction.

For the 100-year rain event, lower degrees of implementation result in greater flood reduction relative to the connected impervious area provided the drainage system is moderately overloaded. If the drainage system is overloaded far beyond its capacity, as in the

100 mm rain event, the reduction in flood volume is linear to the NBS implementation degree. With a high-capacity drainage system, even lower degrees of NBS implementation make a significant contribution to flood reduction. The authors are aware that implementation degrees of just 25% are almost impossible to achieve in existing inner-city areas. The following facts were neglected, i.e., if there is green space for infiltration systems in the vicinity of roofs available and whether roofs or tree locations can be converted into green roofs, tree pits, or tree trenches. However, in this study, the potential of NBSs is the focus of why certain limitations are overlooked.

The comparison of the NBSs for flood mitigation reveals that infiltration systems dimensioned to T = 5 and 100 a can significantly reduce flooding for R1E. With R2E, the effectiveness of the systems Type 5 a declines significantly. It is widely known in the literature that the effectiveness of NBSs for flood mitigation decreases with more intense rain events [15,16,27]. However, infiltration systems of Type 100 a can still effectively reduce flooding and achieve almost three times the flood reduction compared to systems such as Type 5 a. The extension of infiltration systems beyond their usual dimensioning significantly increases the resilience of urban drainage systems in case of extreme heavy rainfall events. For maximum flood mitigation, swale–trench–elements are recommended. If no free green space is available, infiltration trenches can be used. Overall, green roofs have the biggest effect on flood reduction, with the retention roofs fully detaining R2E and the extensive green roofs almost detaining the event. The performance of extensive green roofs comes close to swales dimensioned to T = 100 a. If the structural design of roofs allows them to be converted to green roofs, these can significantly contribute to flood protection during extreme heavy rainfall events. However, in this study, only event-based simulations were conducted, but the performance of green roofs is determined by the water content of the soil layer, which depends on previous rainfall and evapotranspiration. Both of these factors have been neglected in this study. For future research, long-term simulations with appropriate consideration of evapotranspiration are needed. The tree pits and tree trenches are both dimensioned to T = 5 a and have the least effect on flood reduction. However, rainfall events up to a return period of T = 100 a can be used in combination with other NBSs: roof areas are connected to swales, and the runoff from street areas is conveyed to the tree locations.

The selected rainfall distribution significantly impacts flooding in the study area. The peak intensity of the Euler type 2 rainfall results in higher maximum flood heights, which is more pronounced in the base model than in the models with NBSs. The relative differences in flood volume are quite similar when comparing the NBSs, suggesting that the NBSs react similarly to the different rainfall distributions. The rainfall duration has a major influence on the performance of infiltration systems. The proportion of runoff that is infiltrated increases with the duration of the rainfall. However, this depends on the infiltration capacity of the soil.

The arrangement of the NBSs in the study area has a major influence on the inundation heights in the center of flooding. The NBSs should be centered around the flooding area for maximum flood protection. Webber et al. support these findings, stating that local NBS strategies can delay flood peaks in areas of severe flooding [27].

However, it is essential to note that the results of this study are only transferable to a limited extent. The occurrence of flooding in an area depends heavily on the topography and the performance of the urban drainage system, which are unique to each catchment. This study presents the results of a study area with a very flat topography. For this reason, the investigations will be carried out in a second, steeper study area, and the results will be compared. Additionally, the impact of additional NBSs on flood mitigation, such as rainwater harvesting tanks, should be analyzed.

5. Conclusions

This study presented a method to implement NBSs in a 1D/2D coupled model to evaluate their potential for flood mitigation. Their effectiveness in flood reduction in different infiltration systems, green roofs, and tree locations was compared and evaluated based on design rains with varying return periods, durations, and rainfall distributions. Additionally, the influence of the spatial distribution of NBSs in the study area was investigated. The following more general qualitative conclusions can be drawn from these case-specific quantitative results.

While the effect of NBSs declines with an increase in rainfall intensity, infiltration systems dimensioned to 100 years still have a major effect on flood reduction, even for extreme rainfall events. Overall, the intensive green and the retention roof have the biggest effect on flood reduction. The performance of the extensive green roof comes close to a swale dimensioned to a return period of 100 years. The tree trenches and tree pits have the least effect on flood mitigation but can be combined with other NBSs. No additional space is used if a retrofit of existing street trees to tree pits is possible.

The rainfall characteristic has a major influence on flooding, but the NBSs are robust for different rainfall distributions. During long durations of rainfall, the effectiveness of infiltration systems increases. For maximum flood protection, the NBSs should be located around the center of flooding.

Long-term simulations that appropriately consider evapotranspiration are needed for future research to model the NBS system behavior more realistically.

Author Contributions: Conceptualization, U.D., C.S. and J.N.; methodology, J.N. and C.S.; software, J.N.; formal analysis, J.N.; investigation, J.N.; resources, U.D.; data curation, J.N.; writing—original draft preparation, J.N.; writing—review and editing, U.D. and C.S.; visualization, J.N.; supervision, U.D.; project administration, C.S.; funding acquisition, U.D., C.S. and J.N. All authors have read and agreed to the published version of the manuscript.

Funding: This research was funded by the German Federal Ministry of Education and Research (BMBF) under the funding code 02WEE1624 as a part of the WaX (Water Extreme Events) funding program for the project AMAREX. The authors would like to express their sincere thanks for this project funding.

Data Availability Statement: The geo data from the study area are available from the geoportal of Berlin (FIS-Broker), except for the 1D sewer data and the yard, walk, and bike areas due to privacy reasons.

Acknowledgments: The authors would like to thank Berliner Wasserbetriebe, the municipal water services of Berlin, for providing the data for the development of the model.

Conflicts of Interest: The authors declare no conflicts of interest.

Appendix A

Table A1. KOSTRA-DWD-2020 data for grid field 105190 (location of the study area).

	Precipitation Height [mm] in Dependence of the Return Period [Years]						
Duration [min]	**1**	**5**	**10**	**20**	**30**	**50**	**100**
5	6.3	10.6	12.7	14.8	16.2	18.1	20.7
10	8.5	14.4	17.2	20.1	22	24.6	28.1
15	9.8	16.7	20	23.3	25.6	28.5	32.6
20	10.8	18.3	21.9	25.7	28.1	31.3	35.9
30	12.2	20.7	24.8	29	31.8	35.4	40.5
45	13.7	23.2	27.7	32.5	35.5	39.6	45.4
60	14.8	25	29.9	35	38.3	42.7	48.9
90	16.3	27.7	33.1	38.7	42.4	47.2	54.1
120	17.5	29.7	35.5	41.5	45.5	50.7	58.1
180	19.3	32.6	39.1	45.7	50.1	55.8	63.9

Table A2. Simulation runs with homogenous NBS distribution; S: swale, IT: infiltration trench, STE: swale–trench–element, EGR: extensive green roof, IGR: intensive green roof, RR: retention roof, TP: tree pit, and TT: tree trench.

Rain Fall Load	Degree of Implementation	Base Model	Infiltration Systems						Green Roofs			Tree Locations	
			S		IT		STE		EGR	IGR	RR	TP	TT
			5 a	100 a	5 a	100 a	5 a	100 a	-	-	-	5 a	5 a
R1E Euler type 2	-	x	-	-	-	-	-	-	-	-	-	x	x
	25%	-	x	x	x	x	x	x	x	x	x	-	-
	50%	-	x	x	x	x	x	x	x	x	x	-	-
	75%	-	x	x	x	x	x	x	x	x	x	-	-
	100%	-	x	x	x	x	x	x	x	x	x	x	x
	50.3%	-	-	-	-	-	-	-	-	-	x	-	-
R2E Euler type 2	-	x	-	-	-	-	-	-	-	-	-	x	x
	25%	-	x	x	x	x	x	x	x	x	x	-	-
	50%	-	x	x	x	x	x	x	x	x	x	-	-
	75%	-	x	x	x	x	x	x	x	x	x	-	-
	100%	-	x	x	x	x	x	x	x	x	x	x	x
	50.3%	-	-	-	-	-	-	-	-	-	x	-	-
R1B Block rain	-	x	-	-	-	-	-	-	-	-	-	-	-
	100%	-	x	x	x	x	x	x	x	x	x	-	-
R1E6 Euler type 2	-	x	-	-	-	-	-	-	-	-	-	-	-
	100%	-	x	x	x	x	x	x	x	x	x	-	-

References

1. IPCC. *Climate Change 2023: Synthesis Report. Contribution of Working Groups I, II and III to the Sixth Assessment Report of the Intergovernmental Panel on Climate Change*; Core Writing Team, Lee, H., Romero, J., Eds.; IPCC: Geneva, Switzerland, 2023; 184p. [CrossRef]
2. Westra, S.; Fowler, H.; Evans, J.; Alexander, L.; Berg, P.; Johnson, F.; Kendon, E.; Lenderink, G.; Roberts, N. Future changes to the intensity and frequency of short-duration extreme rainfall. *Rev. Geophys.* **2014**, *52*, 522–555. [CrossRef]
3. Share of Urban Population Worldwide in 2023, by Continent—Statista. Available online: https://www.statista.com/statistics/270860/urbanization-by-continent/ (accessed on 16 January 2024).
4. The Largest Cities Worldwide 2023—Statistisches Bundesamt Deutschland (Destatis). Available online: https://www.destatis.de/EN/Themes/Countries-Regions/International-Statistics/Data-Topic/Population-Labour-Social-Issues/DemographyMigration/UrbanPopulation.html#:~:text=International%20statistics%20The%20largest%20cities%20worldwide%202023&text=Mid-2023%20approximately%204.6%20of,57%25%20of%20the%20global%20population (accessed on 16 January 2024).
5. Fletcher, T.; Shuster, W.; Hunt, W.; Ashley, R.; Butler, D.; Arthur, S.; Trowsdale, S.; Barraud, S.; Semadeni-Davies, A.; Bertrand-Krajewski, J.-L.; et al. SUDS, LID, BMPs, WSUD and more—The evolution and application of terminology surrounding urban drainage. *Urban Water J.* **2015**, *12*, 525–542. [CrossRef]
6. Schmitt, T.; Thomas, M.; Ettrich, N. Analysis and modeling of flooding in urban drainage systems. *J. Hydrol.* **2004**, *299*, 300–311. [CrossRef]
7. Butler, D.; Ward, S.; Sweetapple, C.; Astaraie-Imani, M.; Diao, K.; Farmani, R.; Fu, G. Reliable, resilient and sustainable water management: The Safe & SuRe approach. *Glob. Chall.* **2017**, *1*, 63–77. [CrossRef] [PubMed]
8. O'Hogain, S.; McCarton, L. *A Technology Portfolio of Nature Based Solutions*, 1st ed.; Springer International Publishing: Cham, Switzerland, 2018.
9. Definition NBS—European Comission. Available online: https://research-and-innovation.ec.europa.eu/research-area/environment/nature-based-solutions_en (accessed on 17 January 2024).
10. Shafique, M.; Kim, R. Application of green blue roof to mitigate heat island phenomena and resilient to climate change in urban areas: A case study from Seoul, Korea. *J. Water Land Dev.* **2017**, *33*, 165–170. [CrossRef]
11. Cirkel, D.; Voortman, B.; van Veen, T.; Bartholomeus, R. Evaporation from (Blue-)Green Roofs: Assessing the Benefits of a Storage and Capillary Irrigation System Based on Measurements and Modeling. *Water* **2018**, *10*, 1253. [CrossRef]
12. Schneider, F.; Helmreich, B.; Gelhar, T. Bemessungsansätze für Versickerungsanlagen im internationalen Vergleich, Teil 1: Bemessungsansätze in unterschiedlichen Ländern. *KA Korrespondenz Abwasser Abfall* **2017**, *17*, 22–23.
13. Almaaitah, T.; Appleby, M.; Rosenblat, H.; Drake, J.; Joksimovic, D. The potential of Blue-Green infrastructure as a climate change adaptation strategy: A systematic literature review. *Blue-Green Syst.* **2021**, *3*, 223–248. [CrossRef]
14. Rossman, L.A.; Simon, M.A. *Storm Water Management Model User's Manual, version 5.2*; U.S. Environmental Protection Agency (EPA): Cincinnati, OH, USA, 2022.
15. Ortega Sandoval, A.; Sörensen, J.; Rodríguez, J.; Bharati, L. Hydrologic-hydraulic assessment of SUDS control capacity using different modeling approaches: A case study in Bogotá, Colombia. *Water Sci. Technol.* **2023**, *87*, 3124–3145. [CrossRef]

16. Mu, J.; Huang, M.; Hao, X.; Chen, X.; Yu, H.; Wu, B. Study on Waterlogging Reduction Effect of LID Facilities in Collapsible Loess Area Based on Coupled 1D and 2D Hydrodynamic Model. *Water* **2022**, *14*, 3880. [CrossRef]
17. Iffland, R.; Förster, K.; Westerholt, D.; Pesci, M.; Lösken, G. Robust Vegetation Parameterization for Green Roofs in the EPA Stormwater Management Model (SWMM). *Hydrology* **2021**, *8*, 12. [CrossRef]
18. Lisenbee, W.; Hathaway, J.; Winston, R. Modeling bioretention hydrology: Quantifying the performance of DRAINMOD-Urban and the SWMM LID module. *J. Hydrol.* **2022**, *612*, 128179. [CrossRef]
19. Gülbaz, S.; Kazezyılmaz-Alhan, C. An evaluation of hydrologic modeling performance of EPA SWMM for bioretention. *Water Sci. Technol.* **2017**, *76*, 3035–3043. [CrossRef] [PubMed]
20. Chang, T.-J.; Wang, C.-H.; Chen, A. A novel approach to model dynamic flow interactions between storm sewer system and overland surface for different land covers in urban areas. *J. Hydrol.* **2015**, *524*, 662–679. [CrossRef]
21. Blanc, J.; Hall, J.; Roche, N.; Dawson, R.; Cesses, Y.; Burton, A.; Kilsby, C. Enhanced efficiency of pluvial flood risk estimation in urban areas using spatial–temporal rainfall simulations. *J. Flood Risk Manag.* **2012**, *5*, 143–152. [CrossRef]
22. Hamers, E.; Maier, H.; Zecchin, A.; van Delden, H. Effectiveness of Nature-Based Solutions for Mitigating the Impact of Pluvial Flooding in Urban Areas at the Regional Scale. *Water* **2023**, *15*, 642. [CrossRef]
23. Bae, C.; Lee, D. Effects of low-impact development practices for flood events at the catchment scale in a highly developed urban area. *Int. J. Disaster Risk Reduct.* **2020**, *44*, 101412. [CrossRef]
24. Haghighatafshar, S.; Nordlöf, B.; Roldin, M.; Gustafsson, L.-G.; La Cour Jansen, J.; Jönsson, K. Efficiency of blue-green stormwater retrofits for flood mitigation—Conclusions drawn from a case study in Malmö, Sweden. *J. Environ. Manag.* **2018**, *207*, 60–69. [CrossRef]
25. Bai, Y.; Zhao, N.; Zhang, R.; Zeng, X. Storm Water Management of Low Impact Development in Urban Areas Based on SWMM. *Water* **2019**, *11*, 33. [CrossRef]
26. Costa, S.; Peters, R.; Martins, R.; Postmes, L.; Keizer, J.; Roebeling, P. Effectiveness of Nature-Based Solutions on Pluvial Flood Hazard Mitigation: The Case Study of the City of Eindhoven (The Netherlands). *Resources* **2021**, *10*, 24. [CrossRef]
27. Webber, J.; Fletcher, T.; Cunningham, L.; Fu, G.; Butler, D.; Burns, M. Is green infrastructure a viable strategy for managing urban surface water flooding? *Urban Water J.* **2020**, *17*, 598–608. [CrossRef]
28. Mugume, S.; Kibibi, H.; Sorensen, J.; Butler, D. Can Blue-Green Infrastructure enhance resilience in urban drainage systems during failure conditions? *Water Sci. Technol.* **2024**, *89*, 915–944. [CrossRef]
29. FIS-Broker—Senate Department for Urban Development, Building and Housing (SenBW). Available online: https://fbinter.stadt-berlin.de/fb/index.jsp (accessed on 17 January 2024).
30. DWA. *DWA-A 138-1, Entwurf. Teil 1: Planung, Bau, Betrieb Anlagen zur Versickerung von Niederschlagswasser*; Deutsche Vereinigung für Wasserwirtschaft Abwasser und Abfall: Hennef, Germany, 2020.
31. Hürter, H. *Erarbeitung Gebietsspezifischer Anwendungsempfehlungen für Bi-Direktional Gekoppelte 1D-2D-Überflutungsberechnungen*; Fachbereich Bauingenieurwesen: Kaiserslautern, Germany, 2018.
32. Sieker, F. On-site stormwater management as an alternative to conventional sewer systems: A new concept spreading in Germany. *Water Sci. Technol.* **1998**, *38*, 65–71. [CrossRef]
33. BlueGreenStreets. *BlueGreenStreets Toolbox—Teil A & B. Multifunktionale Straßenraumgestaltung Urbaner Quartiere*; Erstellt im Rahmen der BMBF-Fördermaßnahme "Ressourceneffiziente Stadtquartiere für die Zukunft" (RES:Z); HafenCity Universität Hamburg: Hamburg, Germany, 2022.
34. FLL. *Dachbegrünungsrichtlinien—Richtlinien für Planung, Bau und Instandhaltung von Dachbegrünungen*; Forschungsgesellschaft Landschaftsentwicklung Landschaftsbau e.V.: Bonn, Germany, 2018.
35. FLL. *Empfehlungen für Baumpflanzungen. Teil 2: Standortvorbereitungen für Neupflanzungen*; Pflanzgruben und Wurzelraumerweiterung, Bauweisen und Substrate, Forschungsgesellschaft Landschaftsentwicklung Landschaftsbau e.V.: Bonn, Germany, 2010.
36. Rossman, L.A.; Huber, W.C. *Storm Water Management Model Reference Manual Volume III—Water Quality*; U.S. Environmental Protection Agency (EPA): Cinncinati, OH, USA, 2016.
37. Rawls, W.J.; Brakensiek, D.I.; Miller, N. Green Ampt Infiltration Parameters from Soils Data. 1983. Available online: http://soilphysics.okstate.edu/teaching/soil-6583/references-folder/rawls%20et%20al%201983.pdf (accessed on 17 January 2024).
38. Peng, Z.; Stovin, V. Independent Validation of the SWMM Green Roof Module. *J. Hydrol. Eng.* **2017**, *22*, 1–12. [CrossRef]
39. Jeffers, S.; Garner, B.; Hidalgo, D.; Daoularis, D.; Warmerdam, O. Insights into green roof modeling using SWMM LID controls for detention-based designs. *J. Water Manag. Model.* **2022**, *30*, C484. [CrossRef]
40. KOSTRA-DWD-2020 Datensatz—Deutscher Wetterdienst. Available online: https://opendata.dwd.de/climate_environment/CDC/grids_germany/return_periods/precipitation/KOSTRA/KOSTRA_DWD_2020/gis/ (accessed on 17 January 2024).